

## Solvent driven phase transitions of acyclovir – the role of water and solvent polarity

Karol P. Nartowski<sup>a,b,\*</sup>, Julia Karabin<sup>a</sup>, Alexander L. Morrirt<sup>b</sup>, Maciej Nowak<sup>a</sup>, László Fábián<sup>b</sup>, Bożena Karolewicz<sup>a</sup>, Yaroslav Z. Khimyak<sup>b,\*</sup>

Received 00th January 20xx,  
Accepted 00th January 20xx

DOI: 10.1039/x0xx00000x

www.rsc.org/

Acyclovir, an antiviral purine derivative listed on the WHO Model List of Essential Medicines, is commonly used in several different dosage forms from tablets to gels, oleogels and suspensions. Although temperature driven phase transitions of its commercially available 3:2 hydrate have been known since 2011, information on the solvent driven phase transitions of this drug has been limited. This study identifies the pathways of transformations of acyclovir forms I and V induced by organic solvents and water using the method of solution mediated phase transformation. The 3:2 hydrate, form V, undergoes dehydration to anhydrous form I in methanol, ethanol and N,N-dimethylformamide. Form I converts to anhydrous form II in dry methanol and N,N-dimethylformamide, while increased water content in the solvent prevents the transformation of form I to form II. Both forms I and V yield a gel-like material in dimethyl sulfoxide, composed of highly crystalline form II and reported here for the first time. Furthermore, significant differences in the thermal dehydration process of forms V and VI were observed using VT FTIR, including the first time report on a novel metastable ACV form VII formed upon dehydration of ACV dihydrate (form VI). High resolution solid-state NMR spectra of two anhydrous polymorphs (forms I and II) and two hydrates (forms V and VI) supported by DFT calculations using the CASTEP code are also presented.

### Introduction

Acyclovir, (ACV, 2-amino-1,9-dihydro-9-[(2-hydroxyethoxy)methyl]-6H-purin-6-on) a guanine derivative, is an important antiviral drug listed on the WHO Model List of Essential Medicines (Figure 1A). ACV belongs to BCS class III (Biopharmaceutical Classification System) indicating the drug to be soluble in water but to have limited permeability.<sup>1</sup> This is in line with its limited bioavailability (5 to 30%), which varies between individuals.<sup>2</sup> Furthermore, it is known that different ACV solid forms display substantial differences in dissolution kinetics, which may affect the bioavailability of the drug.<sup>2,3</sup>

ACV can form varied hydrogen bonding networks due to the presence of eight potential hydrogen donors/acceptors and a flexible side chain, which results in four polymorphs and two hydrate forms reported to date. The reported crystalline phases were obtained using polymer-induced heteronucleation (PIHn) and at increased temperatures by Lutker *et al.*<sup>4</sup> and through the application of dynamic vapour sorption by Terada *et al.* (Figure 1B, ESI Figure S11).<sup>5</sup>

Based on the studies of Lutker *et al.*<sup>4</sup> and Terada *et al.*<sup>5</sup> ACV forms two hydrates – the commercially available 3:2 ACV:water

hydrate (form V) and a 1:2 dihydrate (form VI), two anhydrous forms, I and II, and two forms stable only at high temperature, forms III and IV.<sup>4</sup> ACV form V was first reported by Birnbaum *et al.* in 1980s.<sup>6,7</sup> The anhydrous ACV form I (nomenclature proposed by Lutker *et al.*<sup>4</sup>) can be obtained by heating the commercial form (form V) to 180 °C followed by cooling to room temperature or via crystallization of acyclovir from methanol in the presence of the polymer Nylon 6. The second anhydrous form, ACV form II, can be obtained *via* solution crystallisation of the commercial form of acyclovir in methanol at 68 °C in a closed vial followed by evaporating the solvent under continuous heating<sup>4</sup> or by precipitation from NNDMF using acetonitrile as antisolvent.<sup>5</sup> Dynamic vapor sorption studies carried out by Terada *et al.* have shown that above 90% RH form I transforms into dihydrate (form VI), while form II transforms to 3:2 hydrate (form V) above 95% RH.<sup>5</sup> The metastable anhydrous form III can be obtained by heating the commercial form V between 130 and 150 °C and rapidly returns to the form V during cooling upon exposure to atmospheric water. Further heating of the metastable form III to 180 °C leads to the formation of the high-temperature stable form IV, which after cooling to room temperature undergoes a phase change to form I, which is stable at room temperature.<sup>4</sup> The dihydrate form VI was first obtained during polymorph screening using polymer induced heteronucleation with poly(ethylene terephthalate) and polypropylene (Figure 1B).<sup>4</sup>

<sup>a</sup> Department of Drug Form Technology, Wrocław Medical University, ul. Borowska 211, 50-556 Wrocław, Poland

School of Pharmacy, University of East Anglia, Norwich Research Park, NR4 7TJ Norwich, United Kingdom

\* e-mail addresses: karol.nartowski@umed.wroc.pl and y.khimyak@uea.ac.uk

† Footnotes relating to the title and/or authors should appear here.

Electronic Supplementary Information (ESI) available: See DOI: 10.1039/x0xx00000x

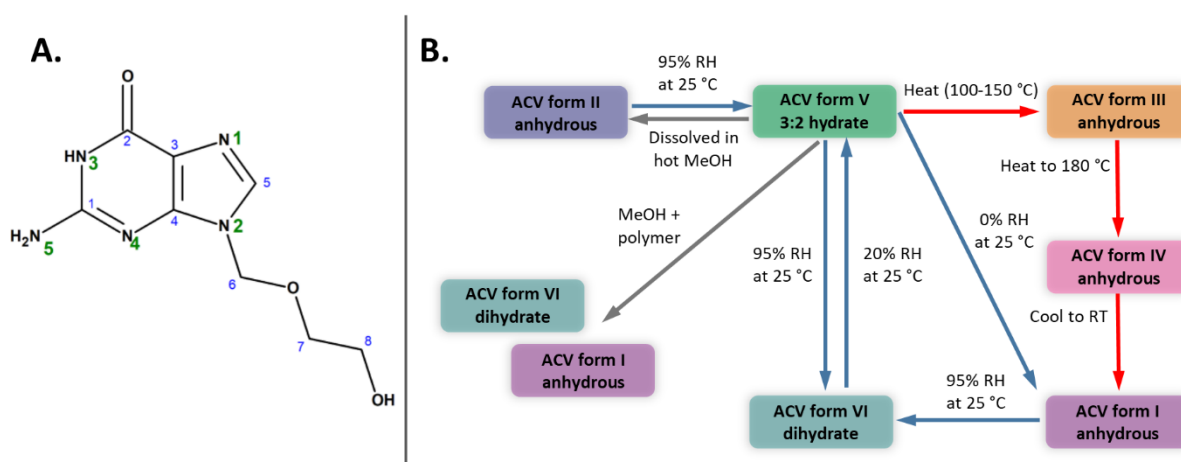


Figure 1. A. Structure of acyclovir with carbon and nitrogen labeling. B. ACV phase transitions described by Terada *et al.* and Lutker *et al.* Blue arrows indicate humidity driven phase transitions, red arrows, temperature driven phase transitions while gray arrows are due to solvent or PIH crystallisation.

Through the analysis of purine ring arrangements in ACV crystal structures, followed by the study of dynamic water sorption, Terada *et al.* proposed explanations for the possible directions of ACV phase transformations. It was shown that form V did not convert to anhydrous form II and anhydrous form I did not undergo direct conversion to form V at 25 °C and RH range of 0-95%. On the other hand, form I could convert to form V only in an indirect way by forming a dihydrate (form VI) at 95% RH and subsequent transformation to form V at 20% RH. This observation was attributed to similar arrangements of the purine rings in the crystal structures of forms I and VI, and the substantial difference in the ring arrangement between the forms I and V. Furthermore, Terada *et al.* hypothesized that anhydrous forms I and II do not undergo direct reciprocal transformation due to different arrangements of the purine rings in both crystal structures.<sup>5</sup> In this manuscript we show that ACV form I undergoes transformation to ACV form II in anhydrous methanol, ethanol, N,N-dimethylformamide and dimethylsulfoxide. To the best of our knowledge, very little is known about solvent induced phase transitions of ACV. This drug is a representative of purine derivatives, a wide group of biologically active substances frequently used in drug discovery and an important group of pharmaceuticals and biologically active molecules essential for all living organisms. Therefore ACV may serve as a model compound to identify solvent effects on the transformations of N-substituted purine derivatives and to help in crystal engineering efforts to expand the solid-state landscape of these compounds.

Polymorph screening is typically carried out by modification of crystallisation conditions *e.g.* temperature, pressure or by using different solvents, which enables the formation of distinct assembly patterns between reacting molecules.<sup>8</sup> Furthermore, as presented by Zhang *et al.*<sup>9</sup> and Gu *et al.*<sup>10</sup> solution mediated phase transformation (SMPT) is an effective method for polymorph screening, including screening for new solvates or cocrystals. This process involves crystallisation or slurring of

the starting material in solvents with different polarities or by the manipulation of the water activity by using a mixture of organic solvents and water.<sup>11-15</sup>

Despite the broad use of acyclovir in a variety of dosage forms, including tablets, gels, creams, oleo gels or suspensions for both systemic and topical treatments, there is limited knowledge available on polymorphic changes driven by solvent. In this work we address this gap by systematic investigation of solvent induced phase transitions of commercially available ACV form V (3:2 ACV:H<sub>2</sub>O hydrate) and anhydrous ACV form I using 15 different solvents. We also report on the effect of hydrate water of ACV hydrate forms V and VI (dihydrate) on the temperature driven dehydration and phase transitions of ACV. Using a combination of state-of-the-art thermal (DSC, TGA), spectroscopic (solid-state NMR, FTIR) and diffraction characterization methods supported by computational NMR crystallography (DFT calculations using CASTEP code) we revisited structural information on some existing forms of ACV, which enabled us to gain a more detailed insight into the thermal desolvation of ACV hydrates and solvent induced transformations of ACV forms I and V. We also report the formation of a new high-temperature phase as the result of the desolvation of form VI. This work describes polymorphic screening and transformations of ACV using a broad range of organic solvents commonly used in the synthesis and drug product development of biologically active substances.

## Experimental

### Materials:

ACV form V was kindly donated by Pharmaceutical Manufacturing Company Hasco-Lek S. A. (Wroclaw, Poland). Solvents of analytical grade used in the study were purchased from Sigma-Aldrich (acetone, 1-propanol, 2-propanol, 1-butanol, ethyl acetate, N,N-dimethylformamide, dimethyl sulfoxide), J. T. Baker (acetonitrile, methanol, ethanol,

dichloromethane, trichloromethane, toluene) and Chemsolve (acetic acid) and used directly without further purification.

#### Methods:

**Recrystallisation of ACV form V.** In order to confirm the polymorphic homogeneity of commercial ACV form V used in the study the received material was compared with freshly prepared ACV form V. 100 mg of ACV form V was dissolved in 40 ml of distilled water at 37 °C and left to recrystallise. The crystals were collected after 24 hours and analysed using PXRD (Powder X-ray Diffraction) and DSC (Differential Scanning Calorimetry).

**Preparation of ACV form I.** The anhydrous form I of ACV was prepared using the method previously described by Lutker *et al.*<sup>4</sup> Briefly, 4.5 g of ACV form V (3:2 hydrate) were spread on a Petri dish and heated in the oven using a heating rate of 5 °C/minute from 25 to 180 °C. The material was left at 180 °C for 30 minutes and then allowed to cool to room temperature. The thermal stability of the drug was confirmed using thermogravimetric analysis. The maximum mass loss observed was 0.4 % after 30 minutes storage of ACV form V at 180 °C (see ESI Figure S1 for details). The obtained ACV form I was analysed directly after preparation.

**Preparation of ACV form II.** The anhydrous form II of ACV was obtained using the following methods: (1) slurry of the ACV form V crystals (3:2 hydrate) in DMSO for at least one week or (2) slurry of anhydrous ACV form I crystals in methanol (MeOH), N,N-dimethylformamide (NNDMF) and dimethyl sulfoxide (DMSO) for 4 weeks in a desiccator over silica gel.

**Preparation of ACV form VI (1:2 ACV:H<sub>2</sub>O dihydrate).** 150 mg of ACV form I was placed into a 10 ml glass vial and gently mixed with 1 ml of distilled water to allow the solvent to cover the surface of the powder. The vial was left at RT (*ca.* 22 °C) for 72 hours. The resulting material was dried on a filter paper prior to analysis.

**Selection of the organic solvents for slurry preparation.** In this study 14 solvents (Table S1) were selected from 7 chemical groups proposed by Gu *et al.*, taking into consideration a variety of solvent properties, including dielectric constant, dipole momentum and propensity of being hydrogen donor or acceptor.<sup>10</sup>

**Preparation of slurries of ACV form I and form V in organic solvents.** The commercial ACV form V (3:2 ACV:H<sub>2</sub>O hydrate) and form I, obtained *via* the dehydration of form V,<sup>4</sup> were used in slurry crystallisation to evaluate the solvent effect on the phase transition of both forms of ACV. For each solvent 300 mg of form V or form I were weighed to a 10 ml glass vial and subsequently, 1.5 mL of a solvent were pipetted into the vial, which was tightly sealed with a cap and protected with Parafilm tape to avoid solvent evaporation and atmospheric water access. Closed vials were then gently mixed to ensure the powder was thoroughly covered by the solvent. The samples

were left at RT (*ca.* 22 °C) for four weeks and then analysed using PXRD, DSC, TGA and FTIR. The materials in which a solid form transformation was observed after 4 weeks of slurrying were prepared again and additionally analysed after 7, 14 and 42 days to evaluate the onset of the transformations in different solvents.

#### Characterisation techniques:

**Fourier-transform infrared spectroscopy.** Room temperature FTIR spectra of the materials were obtained using a Nicolet iS50 FT-IR spectrometer (Thermo Fisher Scientific) using attenuated total reflectance (ATR) mode. The samples were analysed in the wavelength range from 400 to 4000 cm<sup>-1</sup> at 4 cm<sup>-1</sup> resolution. 32 scans were acquired for each material. Variable temperature FTIR analysis was performed using a Bruker Vertex 70 spectrometer with a Specac High Temperature Golden Gate Controller between 30.0 to 250.0 °C.

**Powder X-ray diffraction.** Powder X-ray diffraction patterns were recorded using a Bruker D2 Phaser diffractometer (Bruker AXS, Karlsruhe, Germany) with a LynxEye detector and Cu K $\alpha$  radiation (1.5418 Å) and a low background holder. The samples were surface dried on a filter paper and gently ground using a mortar and pestle. The materials were analysed in the range of 2 $\theta$  from 5° to 36° with 0.02° increment and 1 s/step irradiation time. The optics of the D2 Phaser diffractometer was a 2.5° Soller slit module system, a 0.2 mm divergence slit, a 1 mm air-scatter screen and a Ni filter. The X-ray tube operated at 30 kV and 10 mA.

**Differential scanning calorimetry.** DSC measurements were performed using a Netzsch DSC 214 Polyma calorimeter. The samples were heated in a temperature range from 0 °C to 270 °C with a heating rates of 2; 5; 10 or 20 °C min<sup>-1</sup> using a 50 mL min<sup>-1</sup> purge of dry nitrogen. Depends on the experimental design standard aluminium open, sealed or pin-holed pans sealed using a TA crimper were used in all experiments. The mass of the analysed samples was 5.0  $\pm$  0.5 mg. An empty pin-holed DSC pan was used as a reference.

**Thermogravimetric Analysis.** TGA thermograms were recorded using a Netzsch TG 209 F1 Libra Thermobalance. The mass of the analysed materials was 10.0  $\pm$  0.5 mg. The materials were placed in aluminium oxide crucibles (Al<sub>2</sub>O<sub>3</sub>) and heated from 25.0 to 270.0 °C with a heating rate of 5 °C/min. The obtained thermograms were analysed using the Netzsch Proteus Analysis software.

**Critical Water Activity determination in MeOH and NNDMF.** ACV form I or form V (300 mg) was mixed with methanol/water and NNDMF/water mixtures at different mole fraction of water corresponding to defined water activity (*a<sub>w</sub>*) in the range from 0.007 to 0.26 in MeOH and 0.03 to 0.38 in NNDMF (See section S4 in the ESI for details).<sup>11,16,17</sup> The obtained samples were withdrawn after 7 days of storage at 25.0 °C and the resultant phase was assessed using PXRD. Water content in the residual solutions (without ACV crystals) was determined using coulometric Karl Fischer Titration (Mettler Toledo) according to the protocol described in European Pharmacopoeia.

**Solid-state NMR.**  $^1\text{H}$ - $^{13}\text{C}$  cross-polarization magic angle spinning (CP/MAS) solid-state NMR spectra were acquired using a Bruker Avance III solid-state NMR spectrometer equipped with a triple resonance probe operating at 400.23 MHz for  $^1\text{H}$  and 100.64 MHz for  $^{13}\text{C}$ . Dry powder samples were packed in 4 mm zirconia rotors and rotated at an MAS rate of 10 kHz. The spectra were acquired at 25 °C. The Hartmann–Hahn conditions for  $^1\text{H}$ - $^{13}\text{C}$  CP/MAS experiments were set with hexamethylbenzene (HMB).  $^1\text{H}$ - $^{13}\text{C}$  CP/MAS NMR spectra were acquired using  $^1\text{H}$   $\pi/2$  pulse length of 3.5  $\mu\text{s}$  and  $^1\text{H}$ - $^{13}\text{C}$  contact time of 2000  $\mu\text{s}$ . For each material 384 scans were acquired. Pulse delay was optimised to 10 s. The  $^{13}\text{C}$  chemical shifts were referenced to TMS.

**Computational details.** All computations were performed using the CASTEP code.<sup>18</sup> Chemical shifts were generated for the following crystal structures: ACV I (CSD code: MECWIC01<sup>5</sup>), ACV II (CSD code: MECWIC03<sup>5</sup>), ACV V (CSD code: CEHTAK10<sup>7</sup>) and ACV VI (CSD code: WOZPAE<sup>5</sup>). The geometry optimisation was performed with the Perdew–Burke–Ernzerhof (PBE) generalized gradient approximation (GGA) exchange correlation density functional<sup>19</sup> and ultrasoft pseudopotentials<sup>20</sup> with the Monkhorst-Pack grid sampled with maximum separation of k-points lower than 0.05  $\text{\AA}^{-1}$  and cut-off energy of 800 eV, both optimised for convergence. Geometry optimisation was performed with both cell dimensions and all heavy atom (C, N, O) positions constrained. Chemical shift calculations were performed using the gauge including projector augmented wave approach (GIPAW)<sup>21,22</sup> as implemented in the CASTEP code.

The generated isotropic shielding constants ( $\sigma_{\text{calc}}$ ) were converted to chemical shifts ( $\delta_{\text{calc}}$ ) according to the following equation:  $\delta_{\text{calc}} = \sigma_{\text{ref}} - \sigma_{\text{calc}}$ . The reference shielding constant value ( $\sigma_{\text{ref}}$ ) was taken from the zero intercept of the fit of calculated shielding vs experimental chemical shift plot  $\sigma_{\text{calc}} = -x \cdot \delta_{\text{exp}} + \sigma_{\text{ref}}$ .

## Results and discussion

### Revisiting ACV solid forms

Acyclovir is a N-substituted purine derivative, which has six distinct crystalline structures described to date.<sup>4,5</sup> The rich polymorphism of acyclovir suggests that other biologically active purine derivatives may have a similar, broad solid-state landscape, which is yet to be discovered. Therefore, the detailed characterization of packing motifs and phase transitions of acyclovir driven by temperature or a solvent may serve as a basis for further crystal engineering of this important group of pharmaceutically active compounds.

Four structures of ACV are present in the Cambridge Structural Database (CSD, 2017 version)<sup>23</sup> including two anhydrous forms – ACV form I (CSD ref. code: MECWIC01<sup>5</sup>), ACV form II (CSD ref. code: MECWIC03<sup>5</sup>) and two hydrates – ACV form V *i.e.* 3:2 hydrate (CSD ref. code: CEHTAK10<sup>7</sup>) and ACV form VI *i.e.* dihydrate (CSD ref. code: WOZPAE<sup>5</sup>) (Figure 2, Table 1, ESI Figure S11).

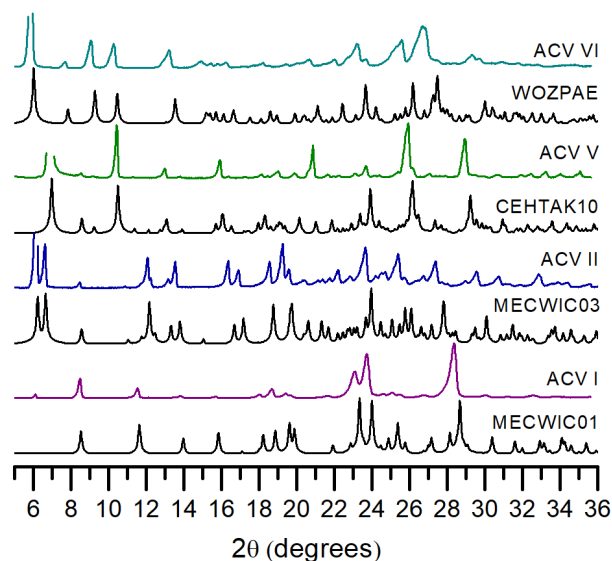


**Figure 2.** Experimental and calculated PXRD patterns of synthesised ACV forms I (CSD ref. code: MECWIC01<sup>5</sup>), II (MECWIC03<sup>5</sup>), V (CEHTAK10<sup>7</sup>), VI (WOZPAE<sup>5</sup>).

The structural characterisation of the ACV solid forms stable at room temperature, including both ACV hydrates (forms V and VI), anhydrous form I and form II *via* the combination of PXRD and solid-state NMR studies supported by computational methods enabled us to further understand the structural rearrangements and polymorphic transformations of ACV. To date only one report has been published on solid-state NMR studies of ACV,<sup>4</sup> in which the presented  $^1\text{H}$ - $^{13}\text{C}$  CP/MAS spectra exhibited several artefacts and significant line broadening. This made the full assignment of different carbon sites and detailed interpretation of the structural information accessible from solid-state NMR very difficult. Herein we present high resolution spectra of ACV polymorphs and hydrates, including the first report on  $^1\text{H}$ - $^{13}\text{C}$  CP/MAS NMR spectrum of ACV form VI.

**Table 1.** Structural data of ACV forms I, II, V and VI.

	Form I	Form II	Form V	Form VI
<b>CSD code</b>	MECWIC01	MECWIC03	CEHTAK10	WOZPAE
<b>Space group</b>	P 2 <sub>1</sub> /c	P 2 <sub>1</sub> 2 <sub>1</sub> 2 <sub>1</sub>	P 2 <sub>1</sub> /n	P-1
<b>Unit cell parameters</b>				
<b>a/Å</b>	10.9402	4.5518	25.459	6.8386
<b>b/Å</b>	11.1854	15.0481	11.282	11.3679
<b>c/Å</b>	8.1167	28.3857	10.768	14.942
<b>α/°</b>	90.0	90.0	90	82.85
<b>β/°</b>	108.63	90.0	95.16	82.42
<b>γ/°</b>	90.0	90.0	90	89.33
<b>Volume, Å<sup>3</sup></b>	941.206	1944.31	3080.34	1142.47
<b>Z</b>	4	8	4	4

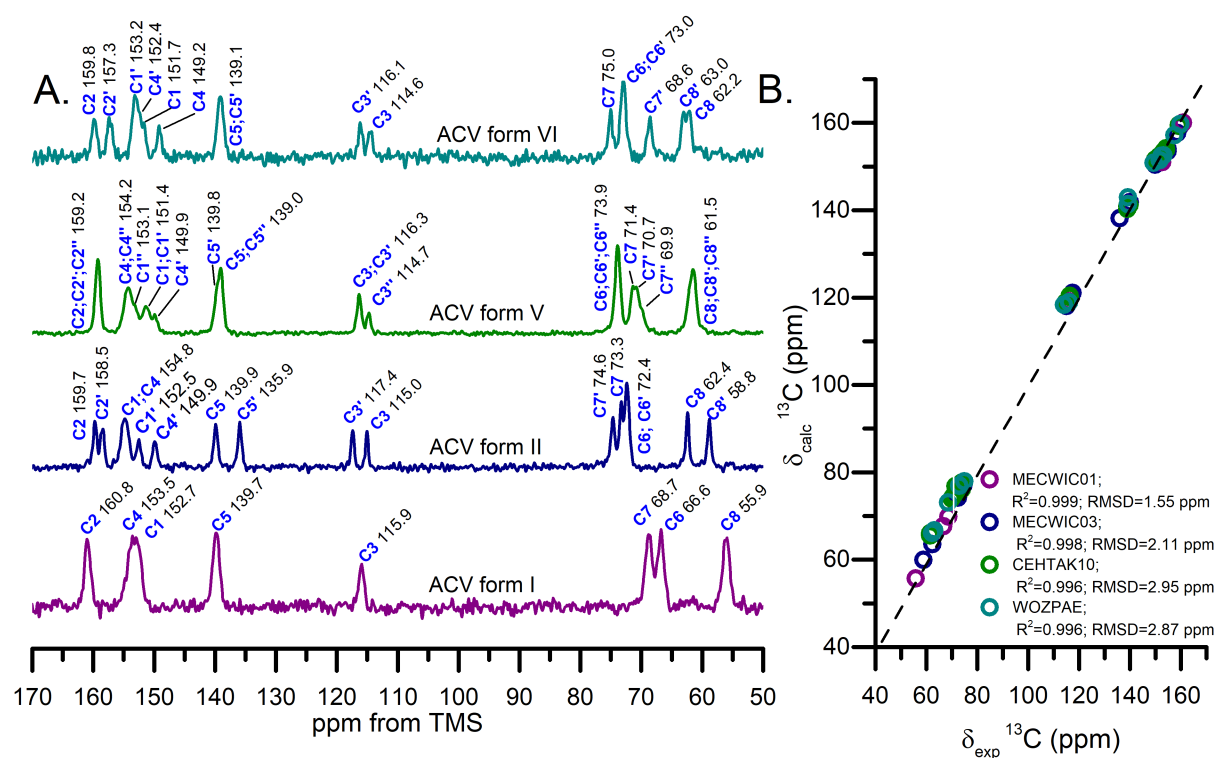


**Figure 3.**  $^1\text{H}$ - $^{13}\text{C}$  CP/MAS NMR spectra of ACV forms I, II, V and VI. B. Comparison of experimental and CASTEP calculated  $^{13}\text{C}$  chemical shifts for ACV forms I (CSD ref. code MECWIC01<sup>5</sup>), II (CSD ref. code MECWIC03<sup>5</sup>), V (CSD ref. code CEHTAK10<sup>7</sup>) and VI (CSD ref. code WOZPAE<sup>5</sup>). The dashed line represents an excellent fit.

The assignment of the  $^1\text{H}$ - $^{13}\text{C}$  CP/MAS solid-state NMR spectra is based on the previously reported spectra<sup>4,24</sup> and CASTEP calculated isotropic chemical shifts (Table S2, Figure 3) for ACV forms I (CSD ref. code: MECWIC01<sup>5</sup>), II (CSD ref. code: MECWIC03<sup>5</sup>), V (CSD ref. code: CEHTAK10<sup>7</sup>) and VI (CSD ref. code: WOZPAE<sup>5</sup>). The commercial form of ACV (form V) is a 3:2 ACV/water hydrate, which crystallises in the  $P2_1/n$  space group and has three molecules of ACV and two molecules of water in the asymmetric unit.<sup>4,5,7</sup> The water molecules are located in channels along the crystallographic  $c$  axis, from where they can be removed by heating the material to 180 °C as first indicated by Lutker *et al.*<sup>4</sup> The simulated PXRD patterns of ACV form V (CSD ref. code: CEHTAK10<sup>7</sup>) are in agreement with experimental PXRD traces of the commercially available material (Figure 2), with characteristic reflections  $d(200) = 12.63$  Å;  $d(210) = 8.44$  Å;  $d(321) = 4.22$  Å and  $d(30-3) = 3.40$  Å. As ACV form V has three ACV molecules in the asymmetric unit, 24 peaks were expected in the  $^1\text{H}$ - $^{13}\text{C}$  CP/MAS solid-state NMR spectrum. The presence of a lower number of peaks (15 peaks) in the spectrum of ACV form V is most likely due to very similar local environments of ACV carbon atoms in the ACV form V structure, resulting in similar values of  $^{13}\text{C}$  chemical shifts. The  $^{13}\text{C}$  peaks of ACV forms are grouped in three distinct regions of the spectrum, *i.e.* peaks of the side chain in the spectral range from 55 to 75 ppm, carbon C3 of the purine ring at ca. 115 ppm and peaks of carbons C1-C5 of the purine ring in the spectral range from 135 to 160 ppm. The detailed description of the spectrum is

presented in ESI Section S7. Despite significant overlapping of the  $^{13}\text{C}$  peaks of ACV form V (*e.g.* carbons C8, C6, C5, C2) the differences in the peak intensities observed in the spectrum of ACV form V support the crystallographic information indicating the presence of three ACV molecules in the unit cell.

Anhydrous ACV form I crystallizes in the  $P2_1/c$  space group with four molecules in the unit cell ( $Z' = 1$ ). The PXRD patterns of ACV form I obtained via dehydration of ACV form V at 180 °C display characteristic peaks  $d(100) = 10.41$  Å;  $d(210) = 4.71$  Å;  $d(20-2) = 3.71$  Å and  $d(30-2) = 3.12$  Å, which are in agreement with calculated PXRD patterns and previously published data (Figure 2).<sup>4,5</sup> The  $^1\text{H}$ - $^{13}\text{C}$  CP/MAS NMR spectrum of ACV form I obtained via dehydration of ACV form V displays significant differences when compared to the starting material (ACV form V). Firstly, there are eight peaks in the spectrum of ACV form I ( $Z' = 1$ ), which can be assigned to the eight carbon atoms of ACV in agreement with the crystallographic data. Secondly, the peaks of the aliphatic side chain carbons C6 and C8 display a *ca.* 5 and 6 ppm up-field shift as compared to ACV form V. This may be explained by the involvement of the side chain of ACV form V in hydrogen bonding. This leads to short contacts between C6 and C8 with electronegative nuclei of neighbouring ACV and water molecules.<sup>25</sup>

As the water oxygens are more electronegative than carbons (and protons) they tend to polarize the electron clouds of neighbouring nuclei towards themselves, which results in the deshielding effects observed. This phenomenon was described

in detail by Spiess *et al.* for ciprofloxacin hydrates using combined application of state of the art solid-state NMR methods and CASTEP calculations.<sup>25</sup> The <sup>13</sup>C peaks of the purine ring of ACV form I undergo only minor changes as compared to the structure of ACV form V. This is consistent with a stacked arrangement of the rings present in both structures and their stabilization *via* similar hydrogen bonding patterns.

The second anhydrous form of ACV (form II) was firstly obtained by crystallisation of ACV from hot methanol with low yield due to the low solubility of ACV in MeOH (0.2 mg/ml).<sup>4</sup> We were able to obtain the same form during solvent-mediated polymorph screening of ACV form I with DMSO, NNDMF and MeOH or ACV form V with DMSO. This phase crystallizes in the  $P2_12_12_1$  space group with two molecules in the asymmetric unit ( $Z = 8$ ). The PXRD pattern of ACV form II displays characteristic peaks with  $d(002) = 14.33 \text{ \AA}$ ;  $d(021) = 7.26 \text{ \AA}$  and  $d(101) = 4.57 \text{ \AA}$  in agreement with the calculated PXRD pattern of the MECWIC03<sup>5</sup> reference structure (Figure 1). Depending on the solvent used for slurry conversion, materials of different crystallinity were obtained, as evidenced by the differences in the broadening of PXRD peaks. The use of MeOH or NNDMF resulted in lower crystallinity, while high crystallinity ACV form II was obtained in DMSO (Figures 8 and 9). The presence of two <sup>13</sup>C peaks for each carbon atom in the spectrum of ACV form II is consistent with there being two molecules in the asymmetric unit. The very different arrangement of ACV molecules in the crystal structures of form I and form II results in different pathways for the phase transitions of these two polymorphs on heating. Form I transforms to the high temperature form IV above 180 °C, while form II does not undergo any phase change before melting (see ESI sections S1 and S2 for details).

Form VI is a dihydrate, with space group symmetry P-1 and two ACV and four water molecules in the asymmetric unit. Its experimental PXRD pattern, with characteristic peaks  $d(001) = 15.04 \text{ \AA}$ ;  $d(011) = 9.7 \text{ \AA}$ ;  $d(012) = 6.63 \text{ \AA}$  and  $d(210) = 3.30 \text{ \AA}$ , is

in agreement with the calculated PXRD pattern for the WOZPAE<sup>5</sup> structure available in the CSD<sup>23</sup> (Table 1, Figure 1). Similarly to ACV form II, the number of peaks in the <sup>1</sup>H-<sup>13</sup>C CP/MAS spectrum of the dihydrate (form VI) is twice the number of carbon atoms in ACV. The unit cell is composed of four ACV molecules, with stacking of the purine rings in alternating orientations, and eight water molecules organised in two channels in close proximity to the aliphatic side chain (see ESI Figure S11). The antiparallel arrangement of stacked purine rings in ACV form VI and form I was used by Terada *et al.* as possible explanation of water sorption induced conversion of form I to the hydrate form VI.<sup>5</sup> The two ACV molecules forming the asymmetric unit of form VI form different hydrogen bonds through their carbonyl oxygen atoms. The carbonyl group of C2 is involved in three hydrogen bonds with two water molecules and an amino group, while the carbonyl group of C2' forms hydrogen bond with one water molecule and an amino group. This is reflected by a slight upfield shift of C2 to 159.7 ppm from 158.5 ppm for C2'.

#### Temperature induced phase transitions of ACV hydrates

The temperature driven phase transitions of acyclovir were first investigated by Lutker *et al.*<sup>4</sup> followed by further structural insights by Terada *et al.*<sup>5</sup> Dehydration and desolvation processes often lead to the formation of crystalline phases that are not readily accessible otherwise. For example, it was demonstrated by our group that the careful removal of methanol from its indomethacin solvate results in the formation of metastable indomethacin form V.<sup>26</sup> Furthermore, the process of removal of the solvent may generate disorder in the crystal lattice, as was demonstrated for the dehydration of orotic acid monohydrate.<sup>15</sup> Here we present the results of the desolvation process of the two ACV hydrate forms, V and VI, based on the combined application of thermal methods (Table 2) and VT FTIR.

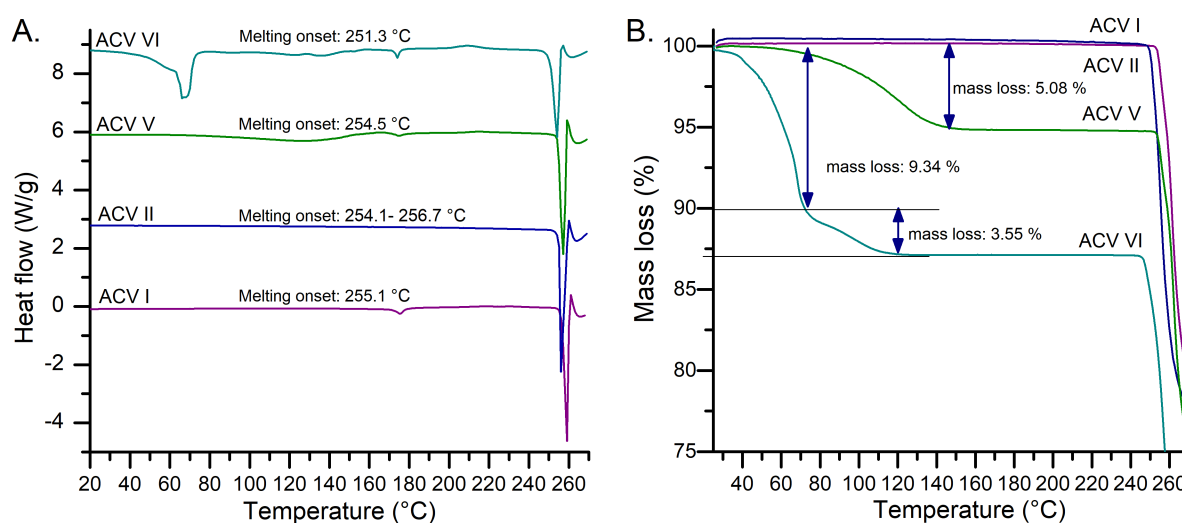


Figure 4. DSC thermograms (A) and TGA curves (B) of ACV forms I, II, V and VI.

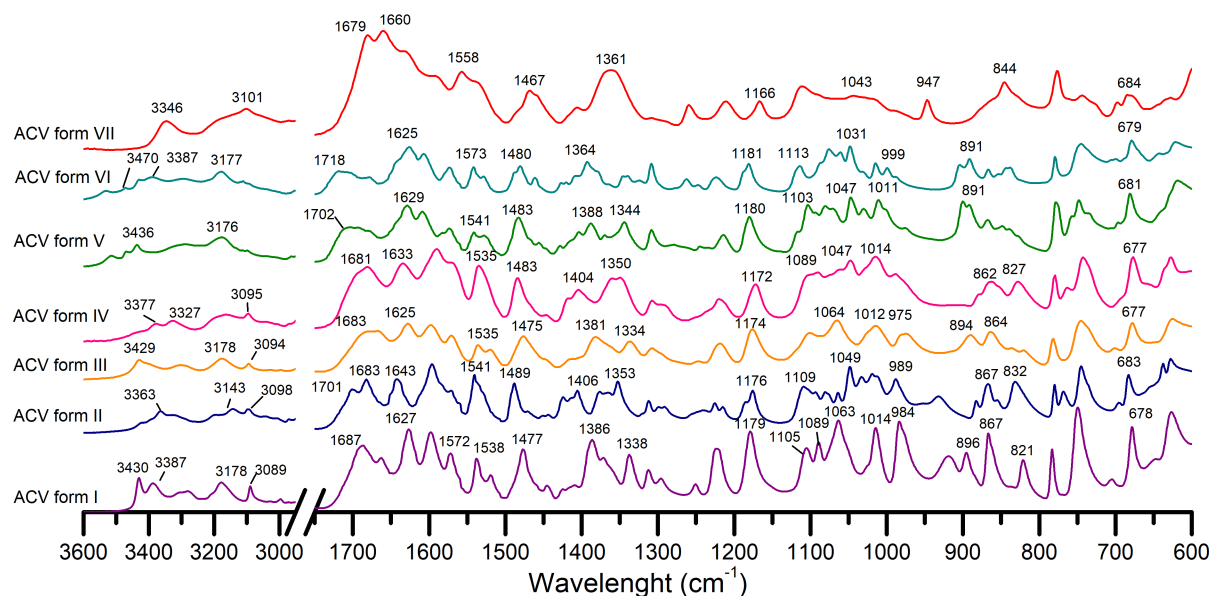
**Table 2.** DSC thermal parameters of ACV forms I, II, V and VI.

ACV form	Unit	Dehydration	Phase transition	Melting onset
ACV I	T [°C]	-	171.0 (ACV form I → IV)	255.1 (ACV form IV)
	ΔH [kJ/mol]	-	2.3	33.5
ACV II	T [°C]	-	-	254.1-256.7 (ACV form II)
	ΔH [kJ/mol]	-	-	33.3-39.5
ACV V	T [°C]	58-155	168.9 (ACV form III → IV)	254.5 (ACV form IV)
	ΔH [kJ/mol]	28.9	2.0	36.3
ACV VI	T [°C]	50-90	173.0 (ACV form V → IV); 200.0 (ACV form IV → VII)	251.3 (ACV form VII)
	ΔH [kJ/mol]	62.4	1.8 4.8	32.3

The DSC curve of form V (3:2 hydrate) shows a broad endothermic peak in the temperature range from 58 to 155 °C (Figure 4A) which corresponds to *ca.* 5.1 % (w/w) loss of water, as confirmed using TGA analysis (Figure 4B). Thermally induced dehydration of ACV form V results in a gradual transition to the metastable form III in the temperature range from 100 to 170 °C, followed by an endothermic transition with an onset at 170.3 °C to the high temperature ACV form IV, as previously described by Lutker *et al.*<sup>4</sup> and confirmed by our group using VT FTIR studies (Figures 5 and 6). Further heating results in melting and decomposition of ACV at 257.1 °C.<sup>4</sup> Cooling of ACV form IV from 180 °C to room temperature results in an exothermic transition to form I, which is stable at room temperature (see ESI Figure S14).

Similarly, to form V, the DSC thermogram (Figure 4A) of anhydrous form I shows an endothermic transition at 171.2 °C corresponding to the formation of form IV as reported by Lutker *et al.* and Terada *et al.* and further confirmed by our group using

VT FTIR (see ESI Figure S15).<sup>4,5</sup> The melting onset and enthalpy of fusion (and decomposition) values of ACV form IV obtained either via heating form V or form I are similar, 254.5 °C (99.70 kJ/mol) and 255.1 °C (97.76 kJ/mol), respectively. In contrast to form I, form II does not undergo any polymorphic transitions on heating, as reflected in the DSC thermogram (Figure 4A). This phase melts within a range of temperatures from 254.1 to 256.7 °C. The DSC thermogram of form VI (dihydrate) shows a complex behavior during heating from room temperature. First an endothermic event is observed in the temperature range between 45 and 70 °C, which is associated with a water loss of *ca.* 10 wt%, while a second broad endotherm in the temperature range from 90 to 160 °C is associated with further weight loss of *ca.* 4 wt% (Figure 4B). The presence of two step water loss is consistent across heating rates used in the TGA experiments (from 2 to 20 °C/min) and indicates that ACV form VI recrystallises to ACV form V, which was confirmed using variable temperature FTIR studies (Figure 6).

**Figure 5.** FTIR spectra of ACV forms I-VII recorded either at RT (forms I, II, V, VI) or extracted from VT experiments (forms III at 175 °C, IV at 230 °C, VII at 250 °C).

The recorded water loss in the first step agrees with the theoretical water loss of form VI to form V transition (i.e. 9.1 %wt). The heating of dihydrate in a closed pan at 5 °C/min shows two peritectic dissociation/transformation processes, first at ca. 66 °C (10.2 kJ/mol) (see ESI Figure S3) followed by a second peritectic dissociation endothermic event at 174 °C. The two endothermic events displayed in the temperature range from 90 to 160 °C when heating in the pierced pan are followed by an endothermic phase transition with an onset at 173.0 °C, which may be related to the formation of form IV. Further heating of the material leads to another exothermic transformation at ca. 210 °C, followed by melting at 251.3 °C (Figure 4).

Due to significant differences in the temperature driven transitions between both ACV hydrates (forms V and VI), we used variable temperature FTIR to further investigate the nature of thermal events observed in the DSC thermograms. The reference FTIR spectra acquired for ACV forms I, II and V agree with FTIR spectra published by Lutker *et al.* Furthermore, VT FTIR studies enabled us to record the previously unknown (to the best of our knowledge) FTIR spectra of the high temperature phases, i.e. forms III, IV and a new high temperature form VII, which was only obtained by heating ACV dihydrate (form VI) above 220 °C. The major spectral differences between the polymorphs of ACV are observed in three main regions: (i) 3600-3000 cm<sup>-1</sup> where NH vibrational bands are observed, (ii) 1750-1650 cm<sup>-1</sup> characteristic of carbonyl stretching and (iii) 1650-1250 cm<sup>-1</sup> arising from alterations in NH bending, C=C and carbonyl stretching and CH bending (Figure 5). ACV form I shows four intense vibrational bands at 3430, 3387, 3187 and 3089 cm<sup>-1</sup> as compared to six low intensity peaks of form II in the spectral range from 3500 to 3000 cm<sup>-1</sup>. Similarly to form II, both ACV hydrates display rather complex spectra with several low intensity peaks in this spectral range. Characteristic for both hydrates are peaks at 3530 (form V), 3513 (form VI) and 3470 cm<sup>-1</sup> (both V and VI), which are not present in anhydrous forms of ACV. Furthermore, the

vibrational bands assigned to the carbonyl groups of hydrates (1750-1650 cm<sup>-1</sup>) are broader, of lower intensity and asymmetrically shifted towards higher wavenumbers (1702 and 1718 cm<sup>-1</sup>) as compared to forms I and II. This may be due to water molecules in the structure forming stronger hydrogen bonds with the carbonyl group, leading to the peak shift towards higher frequencies.<sup>4</sup> The FTIR spectra in the range from 1650 to 1250 cm<sup>-1</sup> of both hydrates and form II are significantly more complex as compared to ACV form I, which may be related to the presence of more than one molecule in the asymmetric unit of these forms.

VT FTIR spectroscopy of ACV form V confirmed the formation of two metastable phases during dehydration of this 3:2 hydrate, i.e. forms III and IV, in agreement with DSC studies and previous research<sup>4,5</sup>. The metastable form III, first observed by Lutker *et al.*<sup>4</sup> and Terada *et al.*<sup>5</sup> upon desolvation of ACV form V, displays similar FTIR spectra to those of form I at temperatures above 120 °C, indicating structural similarity of both phases. This is also corroborated by similarity between VT PXRD patterns of ACV form I and ACV form III presented by Lutker *et al.*<sup>4</sup> and Terada *et al.*<sup>5</sup> Although metastable form III display broadened FTIR peaks, which may be due to the loss of long range ordering upon desolvation, the differences in the spectral regions between 3600 and 3000 cm<sup>-1</sup>, 1700 and 1650 cm<sup>-1</sup> and 1150 to 800 cm<sup>-1</sup> enable us to exclude the possibility of formation of low crystallinity phase I upon desolvation of form V (see ESI Figure S10).

Further heating of the material leads to the formation of the high temperature form IV, with an FTIR spectrum very distinct from form III. This transition is consistent with the phase change observed in the DSC thermogram at ca. 170 °C. Heating of ACV dihydrate (form VI) results in a behaviour very different from form V. The first step of dehydration is observed at ca. 60 °C, leading to form V, as indicated by the FTIR spectra. This observation is similar to the desorption studies performed by Terada *et al.*, in which ACV dihydrate underwent dehydration to ACV 3:2 hydrate at ca. 20% RH.<sup>5</sup>

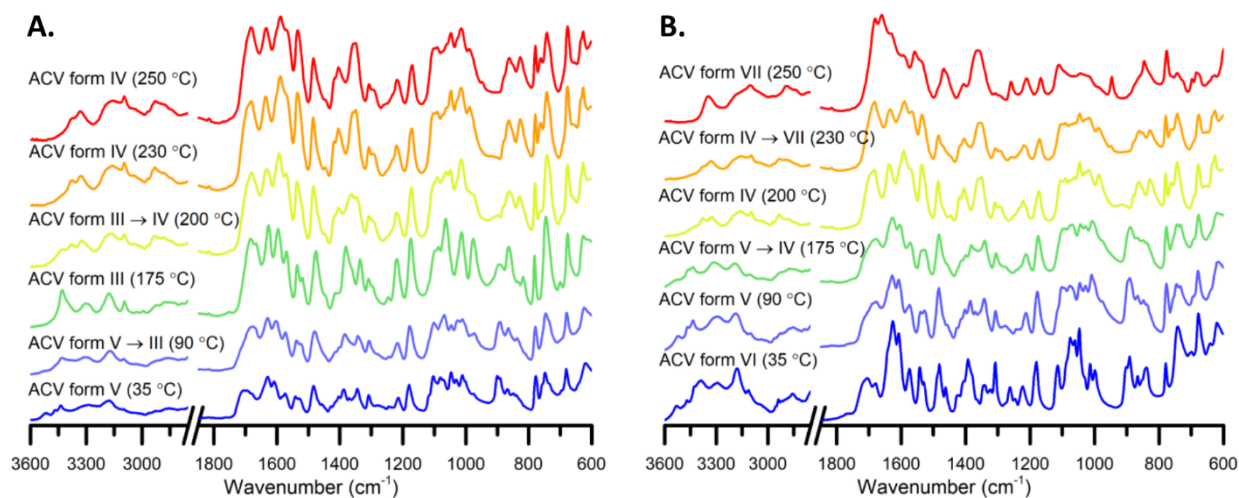


Figure 6. Variable temperature FTIR spectra of A. ACV form V and B. ACV form VI (see also ESI Figure S16).

Interestingly, as observed in the VT FTIR spectra obtained, form V does not undergo any further change until it reaches *ca.* 170 °C. Conversely, the DSC thermograms show that when form V is made from form VI, it undergoes at least two transitions in the temperature range from 100 to 160 °C. This may be related to the water loss observed in the TGA, in a range of temperatures similar to that for form V (Figure 4B). Heating of the material above 210 °C results in further phase change as indicated in the significant changes in the FTIR spectra and corroborated by exothermic event in the DSC thermogram. The observed differences in FTIR peaks broadening between high temperature spectra of forms V and VI may indicate different ordering in both dehydration products. This may affect further transitions of both phases as structural disorder is one of the factors influencing the recrystallisation patterns.

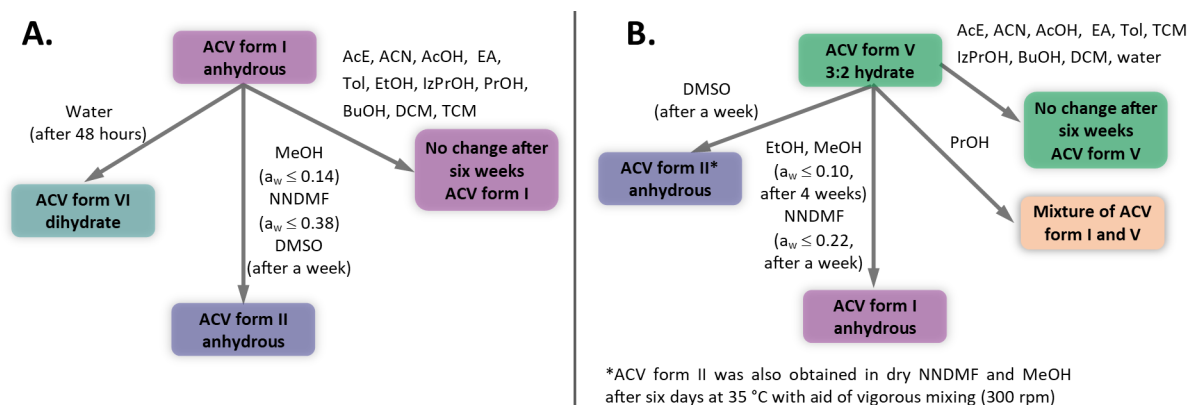
#### Solution-mediated phase transformation of ACV forms V and I – the effect of water

The SMPT is a three-step process – the first stage is the dissolution of the less stable (metastable) form, followed by nucleation and growth of another more stable form.<sup>14,27</sup> Each of the steps may limit the rate of transformation.<sup>14</sup> As indicated by Gu *et al.* a specific polymorphic form of a substance preferentially crystallizes from a specific solvent, even when no seeds of this form are in the crystallization medium. The reason of this phenomenon has been attributed to impact of solvent–solute interactions on the solution mediated polymorphic transformation.<sup>10,14</sup>

To date three studies which describe ACV polymorphism in the context of temperature and humidity driven phase transitions and polymer heteronucleation have been published.<sup>3–5</sup> Although, these studies provide an overview of temperature driven phase transitions and identify several different crystalline structures of this drug, no systematic study of solvent driven phase transitions has been carried out so far. Such study is valuable both in the academic and industrial contexts, as several liquid and semi-solid formulations of ACV are available on the market and significant differences in dissolution kinetics between polymorphs of ACV have been observed.<sup>2,3</sup> ACV form I

slurried in MeOH (at  $a_w \leq 0.14$ ), NNDMF and DMSO results in the formation of form II after one to four weeks (Figure 7), while slurrying in other 11 organic solvents did not result in a phase change (see Scheme 1A, and ESI Figures S26–27). Slurrying of form I in DMSO resulted in the formation of an opaque gel-like material, containing highly crystalline form II (Figure 8 and Figure 9). Transition of form I to form II in MeOH was dependent on water activity (see ESI Section S4). The mixture of forms I, II and V was detected at  $a_w \geq 0.18$  with increasing content of ACV 3:2 hydrate at higher  $a_w (\geq 0.24)$ . The formation of ACV form II in NNDMF was observed at  $a_w \leq 0.38$ .

Slurrying of ACV form V in dry MeOH, EtOH and NNDMF results in dehydration and the formation of form I, which was confirmed by PXRD, FTIR, DSC and TGA (Figure 8, ESI Figures S17–20). The phase change from form V to form I is observed only in dry solvents stored at RH below 40%, which corresponds to  $a_w \leq 0.1$  in MeOH and  $a_w < 0.22$  in NNDMF (see ESI Figures S6 and S7). The increase of water content in the solvent, which may occur upon sorption of water from ambient atmosphere, prevents the form V to form I transition. This phenomenon was most notable for MeOH, in which the phase transition would not occur when stored above 40% RH. Interestingly, once form I is produced in dry MeOH (or EtOH to a lesser extent), an increase of water content in the solvent drives the transition towards the dihydrate form VI (see ESI Figures S18–19), which also can be formed during form I slurrying in water (Figure 7). A mixture of forms I and VI was also obtained by Lutker *et al.* when form V was recrystallised in a mixture of MeOH and Nylon 6 as a source of heteronuclei.<sup>4</sup> The complete transition of form V to form I in NNDMF was observed after the first week of storage, while in EtOH and MeOH the transformation took about four weeks to complete (see ESI Figures S18–19). The quick dehydration of form V in NNDMF may be due to its high water affinity, frequently utilised in dehydration processes in organic synthesis.<sup>28</sup> Slurrying form V in PrOH resulted in a mixture of forms I and V after the first week, which did not undergo any phase change over the next four weeks of the experiment (see ESI Figure S21).



Scheme 1. Solvent mediated phase transitions of ACV forms I (A.) and V (B.).

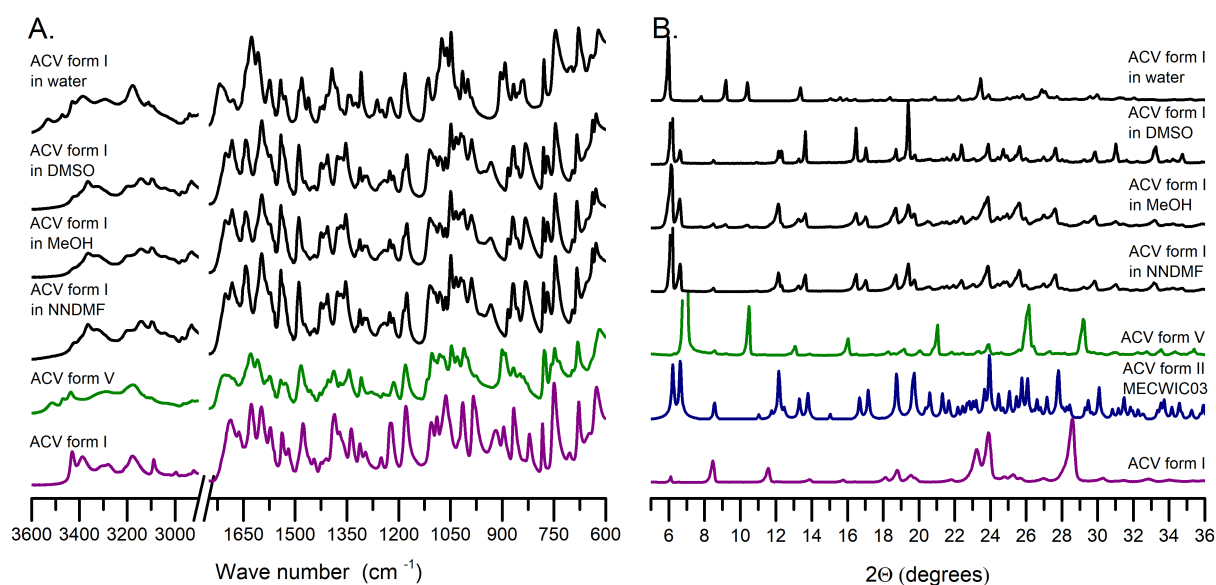


Figure 7. A: FTIR spectra and B. PXRD patterns of ACV form I slurrified for four weeks in NNDMF, MeOH, EtOH, DMSO and water. The FTIR spectra and PXRD patterns of forms I and V along with the calculated PXRD pattern of ACV form II (CSD ref. MECWIC03<sup>5</sup>) are given for comparison.

Slurrifying form V in DMSO resulted in the formation of an opaque, gel-like material composed of high crystallinity ACV form II suspended in the solvent, as confirmed using FTIR, PXRD and solid-state NMR (see Figure 3, Figures 7 and 8 and ESI Figure S22). Slurrifying of form V in nine other organic solvents and water (Scheme 1B) did not produce any phase change during up to six weeks of experimental time (see ESI Figures S21-22). Based on the results of the control experiments of form V slurrifying in MeOH/water and NNDMF/water mixtures at different  $a_w$ , it was demonstrated that transition of form V to

form I is only possible at  $a_w \leq 0.1$  in MeOH and at  $a_w \leq 0.22$  in NNDMF (ESI Figure S7). To verify this further, we performed additional slurry experiments in water, which demonstrated that form I suspended in water forms the dihydrate (form VI) rather than the 3:2 ACV:water hydrate (form V). Furthermore, the addition of seeds of form V to form I suspended in water resulted in a mixture of form V and form VI after a week of storage. This indicates that water drives the transition of form I into dihydrate, even in the presence of the 3:2 ACV:water hydrate, which is the commercially available stable form of ACV.

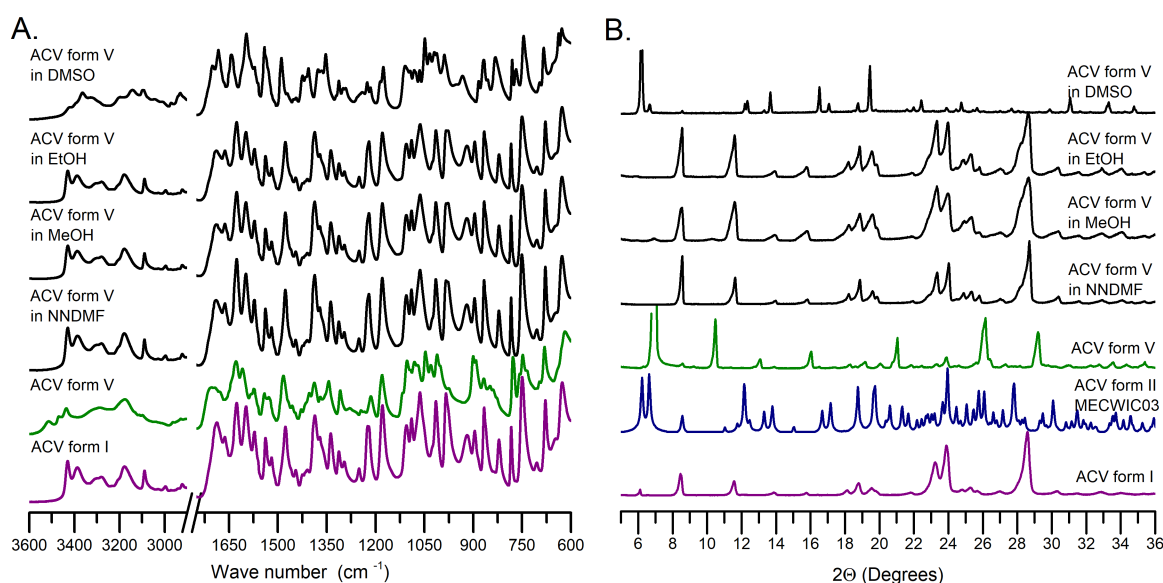


Figure 8. A: FTIR spectra and B. PXRD patterns of ACV form V slurrified for four weeks in NNDMF, MeOH, DMSO and water. The FTIR spectra and PXRD traces of ACV form I and form V along with the calculated PXRD pattern of ACV form II (CSD ref. MECWIC03<sup>5</sup>) are given for comparison.

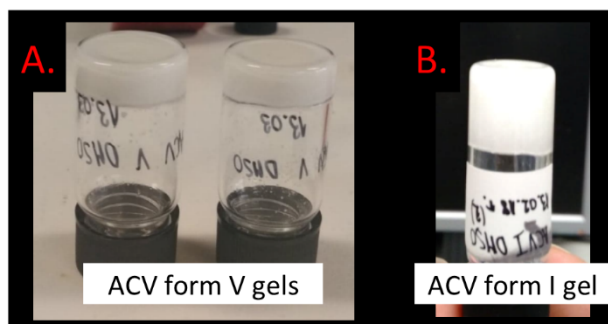


Figure 9. ACV gels in DMSO obtained from ACV form V (A.) and form I (B.)

Despite several attempts the transition from form V to form II in MeOH and NNDMF was never observed during the slurry experiments performed at *ca.* 22 °C (up to 6 weeks of storage). The formation of ACV form II from form V in MeOH and NNDMF was only observed after seeding with form II or in dry solvent after six days of intensive mixing at 35 °C (see ESI Figures S8 and S9). This may be attributed to the much longer time required for the system to equilibrate in the presence of water, which is released to the solution from ACV form V upon transition to form I or to a high energy barrier required to form stable nuclei of form II. In a control experiment ACV form I was slurried in MeOH and NNDMF at  $a_w$  range from 0.03 to 0.38, and after a week of storage traces of ACV form V were detected in MeOH/water mixtures at  $a_w \geq 0.18$  and no phase change to form II was observed. The analysis of the results on form V to form I transformations, in the context of solvent properties, points towards the following characteristics as determining the outcome of the phase transitions. Complete transformations to form I were detected in NNDMF, EtOH and MeOH, while a partial transition was observed in PrOH. Among the selected alcohols used in the slurry experiments, MeOH and EtOH show the highest dielectric constants and values of  $\delta P$  and  $\delta H$  Hansen solubility parameters. Similarly, a high value of dielectric constant (37.22) and  $\delta P$  (13.7) in NNDMF may be correlated with transformation of form V to form I. Therefore, the combination of the high dielectric constant of the solvent (in the range from 20 to 37) with favourable hydrogen bonds and dipolar properties as described using respective Hansen solubility parameters ( $\delta H$  of 11 MPa<sup>0.5</sup>,  $\delta P$  *ca.* 9 MPa<sup>0.5</sup>) may be of importance in determining the outcome of the ACV form V transitions mediated by different solvents. The transformation of form I towards form II in NNDMF, MeOH and DMSO highlight the importance of the high dielectric constant of the solvent required for the phase change. Furthermore, the presence of water in both NNDMF and MeOH blocks this polymorphic transformation. The higher thermodynamic stability of the hydrate forms V and VI in the presence of water may explain the inhibition of the conversion between anhydrous forms I and II, as traces of form VI were observed in the PXRD patterns of ACV form V slurried in MeOH and EtOH after 6 weeks of storage.

**Structural view on the transformations of ACV (Figure 10).** The dehydration of form V (3:2 ACV:water hydrate), the commercially available form of ACV to form I can be performed either via thermal treatment or using organic solvents with high dielectric constant, namely NNDMF (at  $a_w \leq 0.22$ ), EtOH and MeOH (at  $a_w \leq 0.1$ ). The two distinct water molecules present in the crystal structure of form V occupy channels along the *b* axis, partially blocked by the aliphatic chains of ACV molecules. One of the water molecules (Figure 10, blue water molecule) links the hydroxyl groups of two ACV molecules with parallel alignment of their purine rings (Scheme 2, purple and yellow molecules). A third ACV molecule, with an antiparallel alignment of its purine ring (Figure 10, green molecule), is inserted between two parallel ones, forming stacking interactions with both. The same water molecule donates a hydrogen to a carbonyl group (C2=O) of an ACV (yellow) molecule and accepts one from an amino group in neighbouring stacks. The other symmetry-independent water molecule (red) is involved in three hydrogen bonds with three ACV molecules from three different stacks. It donates to a hydroxyl group and a carbonyl group (C2), and accepts from an amino group. Each ACV molecule in the structure forms hydrogen bonded dimers with two neighbouring molecules. The dimers are held together by R<sub>2</sub><sup>2</sup>(9) rings of (amide)N-H...N(imidazole) and NH<sub>2</sub>...O=C2 hydrogen bonds. The molecules in each resulting zig-zag chain have their aliphatic groups pointing in alternating directions. Removal of water from this structure results in form I ( $Z'=1$ ), which presents a very similar chain of ACV dimers to those in form V. On the other hand, the purine rings of stacked ACV molecules in form I display an antiparallel (ABAB) alignment, while in form V two out of three ACV molecules have their purine rings aligned parallel and the third in an antiparallel alignment (AABAAB). Despite form I being formed after dehydration of form V, there are significant differences between both structures indicating the form I is not simply an isomorphous hydrate of form V, but it is formed through other high temperature anhydrous forms or through solvent mediated experiments.

Water molecules in the dihydrate are placed in wide channels along crystallographic *a* axis and form a dense network of hydrogen bonds with each other and with hydroxyl, carbonyl and amino groups of ACV molecules. Pairs of symmetry-independent ACV molecules form hydrogen bonded dimers stabilized by the same hydrogen bonds as in forms V and I. The dimers form chains in a similar way as in forms I and V. The channel structure of the dihydrate explains its rapid, peritectic transformation to the more stable ACV form V upon heating at relatively low temperatures (below 80 °C) as indicated by DSC, TGA and FTIR.

Anhydrous ACV form II, which is formed from form I in MeOH, NNDMF and DMSO and from V in DMSO, shows a different hydrogen bonding pattern from the other known structures of the drug. Each ACV molecule in the structure forms seven hydrogen bonds with three neighbouring molecules.

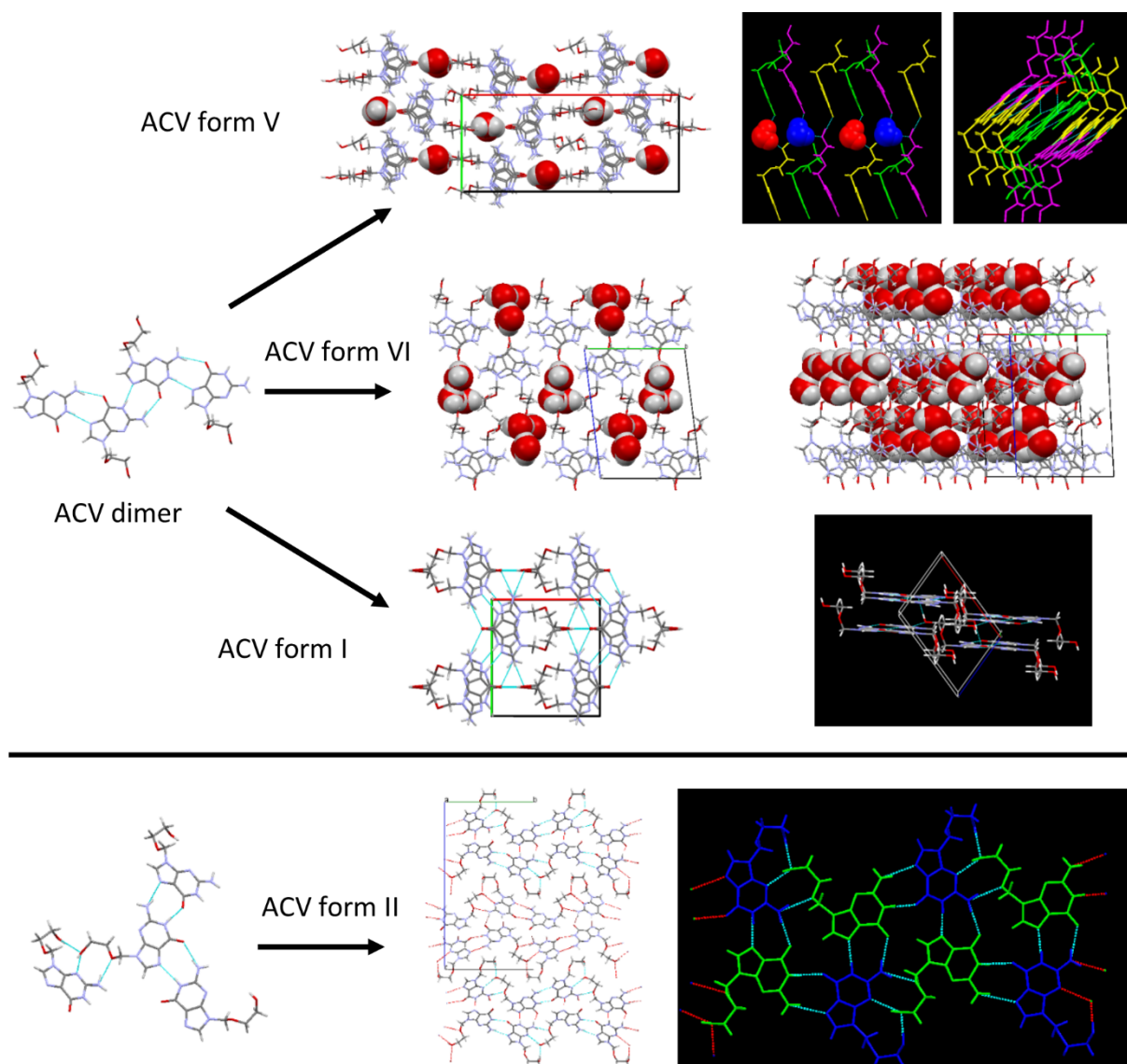


Figure 10. Structural differences between ACV forms. ACV forms V and I are visualised down crystallographic c axis. ACV forms VI and II are visualised down crystallographic a axis. See section: The summary of structural transformations of ACV for details.

The  $R_2^2(9)$  rings of (amide)N-H...N(imidazole) and  $\text{NH}_2\cdots\text{O}=\text{C}2$  hydrogen bonds are still present between symmetry-independent ACV molecules, but are expanded into a complex network by hydroxyl to N(pyrimidine) (green molecules in Figure 10), hydroxyl (blue) to hydroxyl (green) and amino to ether oxygen bonds.

As ACV form II shows significant structural differences from all other forms, it is not surprising that it is not accessible via thermal treatment and only solvent mediated experiments can produce it. The significantly different arrangement of hydrogen bonds requires reformation of the structure via partial dissolution and subsequent nucleation and crystal growth of ACV form II. The performed seeding experiments, in which addition of small amounts of form II crystals to form V or form I slurries, initiated and accelerated the transition towards form II shows that this form is most stable in MeOH and NNDMF.

Transition from form V to form II, which was only observed after addition of the form II seeds, is indicative of a large energy barrier to form stable nuclei of form II or slow kinetics of the process.

## CONCLUSIONS

The systematic investigation of solvent mediated phase transformations of acyclovir performed in 14 organic solvents indicated the dehydration of form V, which results in phase transformation to anhydrous form I is favoured in the highest polarity alcohols (MeOH and EtOH) and NNDMF while form V slurried in DMSO formed a gel-like material composed of crystalline form II. On the other hand, slurrying of form I in highly polar anhydrous MeOH and NNDMF resulted in transition

to form II along with formation of gel-like form II in DMSO. Increased water activity in solvents during slurring experiments of ACV form I prevented the transformation to form II. Combining solution mediated phase transformation experiments with solid-state NMR analysis of obtained solid forms enabled us to gain a more detailed understanding of structural transformations of ACV. This in turn will be beneficial for expanding the knowledge of solid state landscape for N-substituted purine derivatives, an important group of biologically and pharmaceutically active molecules.

## Conflicts of interest

There are no conflicts to declare

## Acknowledgements

The authors acknowledge the use of GRACE High Performance Computing Cluster supported by the Research and Specialist Computing Support service at the University of East Anglia as well as the Faculty of Science Analytical Research Facility. KN, JK and MN would like to thank the Laboratory of Elemental Analysis and Structural Research at the Faculty of Pharmacy at Wrocław Medical University for the access to PXRD, DSC, TG and FTIR instruments. JK and KN would like to thank the Erasmus+ program for financial support for JK research stay at the School of Pharmacy, University of East Anglia.

## REFERENCES

- 1 A. Parr, I. J. Hidalgo, C. Bode, W. Brown, M. Yazdanian, M. A. Gonzalez, K. Sagawa, K. Miller, W. Jiang and E. S. Stippler, *Pharm. Res.*, 2016, **33**, 167–76.
- 2 B. Karolewicz, K. Nartowski, J. Pluta and A. Górniak, *Acta Pharm.*, 2016, **66**, 119–128.
- 3 Y. T. Sohn and S. H. Kim, *Arch. Pharm. Res.*, 2008, **31**, 231–4.
- 4 K. M. Lutker, R. Quiñones, J. Xu, A. Ramamoorthy and A. J. Matzger, *J. Pharm. Sci.*, 2011, **100**, 949–963.
- 5 K. Terada, H. Kurobe, M. Ito, Y. Yoshihashi, E. Yonemochi, K. Fujii and H. Uekusa, *J. Therm. Anal. Calorim.*, 2013, **113**, 1261–1267.
- 6 G. I. Birnbaum, M. Cygler, J. T. Kusmieriek and D. Shugar, *Biochem. Biophys. Res. Commun.*, 1981, **103**, 968–74.
- 7 D. Shugar, G. I. Birnbaum and M. Cygler, *Can. J. Chem.*, 1984, **62**, 2646–2652.
- 8 F. Giordano, *Polymorphism in pharmaceutical solids*, 2001, vol. 71.
- 9 G. G. Z. Zhang, R. F. Henry, T. B. Borchardt and X. Lou, *J. Pharm. Sci.*, 2007, **96**, 990–995.
- 10 C.-H. Gu, H. Li, R. B. Gandhi and K. Raghavan, *Int. J. Pharm.*, 2004, **283**, 117–125.
- 11 H. J. Zhu and D. J. W. Grant, *Int. J. Pharm.*, 1996, **139**, 33–43.
- 12 H. Zhu, C. Yuen and D. J. W. Grant, *Int. J. Pharm.*, 1996, **135**, 151–160.
- 13 Y. Li, P. S. Chow, R. B. H. Tan and S. N. Black, *Org. Process Res. Dev.*, 2008, **12**, 264–270.
- 14 C. H. Gu, V. Young and D. J. W. Grant, *J. Pharm. Sci.*, 2001, **90**, 1878–1890.
- 15 D. E. Braun, K. P. Nartowski, Y. Z. Khimyak, K. R. Morris, S. R. Byrn and U. J. Griesser, *Mol. Pharm.*, 2016, **13**, 1012–1029.
- 16 M. J. Blandamer, J. B. F. N. Engberts, P. T. Gleeson and J. C. R. Reis, *Chem. Soc. Rev.*, 2005, **34**, 440.
- 17 G. Bell, A. E. Janssen and P. J. Halling, *Enzyme Microb. Technol.*, 1997, **20**, 471–477.
- 18 S. J. Clark, M. D. Segall, C. J. Pickard, P. J. Hasnip, M. I. J. Probert, K. Refson and M. C. Payne, *Zeitschrift für Krist.*, 2005, **220**, 567–570.
- 19 J. P. Perdew, K. Burke and M. Ernzerhof, *Phys. Rev. Lett.*, 1996, **77**, 3865–3868.
- 20 D. Vanderbilt, *Phys. Rev. B*, 1990, **41**, 7892–7895.
- 21 C. J. Pickard and F. Mauri, *Phys. Rev. B*, 2001, **63**, 245101.
- 22 J. R. Yates, C. J. Pickard and F. Mauri, *Phys. Rev. B*, 2007, **76**, 024401.
- 23 C. R. Groom, I. J. Bruno, M. P. Lightfoot, S. C. Ward and IUCr, *Acta Crystallogr. Sect. B Struct. Sci. Cryst. Eng. Mater.*, 2016, **72**, 171–179.
- 24 H. Gao and A. K. Mitra, *Magn. Reson. Chem.*, 1999, **37**, 687–689.
- 25 L. Mafra, S. M. Santos, R. Siegel, I. Alves, F. A. Almeida Paz, D. Dudenko and H. W. Spiess, *J. Am. Chem. Soc.*, 2012, **134**, 71–74.
- 26 K. P. Nartowski, J. Tedder, D. E. Braun, L. Fábíán and Y. Z. Khimyak, *Phys. Chem. Chem. Phys.*, 2015, **17**, 24761–24773.
- 27 E. H. Lee, *Asian J. Pharm. Sci.*, 2014, **9**, 163–175.
- 28 S. Ding and N. Jiao, *Angew. Chemie - Int. Ed.*, 2012, **51**, 9226–9237.